Ordered Chiral Structures in the Crystals of Main-Chain Chiral Poly(2-oxazoline)s

ARTICLE *in* MACROMOLECULES · APRIL 2010

Impact Factor: 5.8 · DOI: 10.1021/ma100128q

4654 *Macromolecules* **2010**, *43*, 4654–4659
DOI: 10.1021/ma100128q

Macromolecules
ARTICLE

Ordered Chiral Structures in the Crystals of Main-Chain Chiral Poly(2-oxazoline)s

Meta M. Bloksma,[†,‡,§] Marco M. R. M. Hendrix,[⊥] Ulrich S. Schubert,*[,†,‡,§] and Richard Hoogenboom*[,†,‡]

[†]*Laboratory of Macromolecular Chemistry and Nanoscience, Eindhoven University of Technology, P.O. Box 513, 5600 MB Eindhoven, The Netherlands,* [‡]*Dutch Polymer Institute (DPI), P.O. Box 902, 5600 AX Eindhoven, The Netherlands,* [§]*Laboratory of Organic and Macromolecular Chemistry, Friedrich-Schiller-Universität Jena, Humboldtstrasse 10, 07743 Jena, Germany, and* [⊥]*Materials and Interface Chemistry, Eindhoven University of Technology, P.O. Box 513, 5600 MB Eindhoven, The Netherlands*

Received January 18, 2010; Revised Manuscript Received April 7, 2010

ABSTRACT: The formation of a crystalline structure with the presence of chiral secondary structures was investigated for the enantiopure polymer, p-*R*-2-butyl-4-ethyl-2-oxazoline (p-*R*-BuEtOx), its enantiomer p-*S*-BuEtOx, and the racemic p-*RS*-BuEtOx by differential scanning calorimetry (DSC), X-ray diffraction (XRD), and circular dichroism (CD) of a polymer film. The DSC results revealed that the glass transition temperatures (T_g) of the enantiopure polymers and the racemic polymer are approximately the same with a T_g of ~50 °C. However, the enantiopure polymers showed an additional transition due to cold-crystallization (T_{cc}) followed by two melting peaks (T_{m1} and T_{m2}). Extended thermal investigations indicated that the double melting peak is caused by the melt-recrystallization mechanism. The XRD results confirmed that the enantiopure polymers are semicrystalline and p-*RS*-BuEtOx is amorphous and that no change in crystalline structure appears during the melting transitions. Furthermore, comparison of the DSC results with the CD measurements of the polymer film revealed that the crystals formed during the cold crystallization have an ordered chiral structure, which almost completely disappears during melting.

Introduction

The majority of commercially used polymers like polyethylene (PE) and polypropylene (PP) are semicrystalline polymers.[1] Therefore, it is important to control their crystallization in the solid state.[2] Like PE and PP, poly(2-oxazoline)s[3] can also be semicrystalline depending on the side chain. The thermal properties of a series of poly(2-*n*-alkyl-2-oxazoline)s have already been investigated, revealing that the solid-state properties mainly depend on the side-chain length.[4] Poly(2-oxazoline)s with short alkyl side chains are amorphous polymers, while poly(2-oxazoline)s with longer alkyl side chains are semicrystalline due to side-chain crystallization.[5]

The crystallization of chiral polymers is somewhat more complex since the crystals can contain a secondary structure like helices,[2] which are for example found in isotactic and syndiotactic PP.[6,7] Atactic PP, on the other hand, is amorphous. The exact conformation that is formed in the crystal[6] depends on the degree of stereoregularity and the mechanical and thermal histories of the samples[8,9] as well as the molar mass and polydispersity index.[10] Well-known examples of semicrystalline main-chain chiral polymers are poly(L-lactide) (PLLA) and PDLA, which usually form crystals with a 10_3 helical chain when they are crystallized from the melt or from solution.[11,12] Depending on the melt-crystallization temperature, disordered crystals or imperfect crystals can be formed initially, which transform into ordered or more perfect crystals upon heating.[12,13] The racemic polymer (PDLLA), however, is completely amorphous while a mixture of PDLA with PLLA forms a stereocomplex with a high T_m at 230 °C.[14]

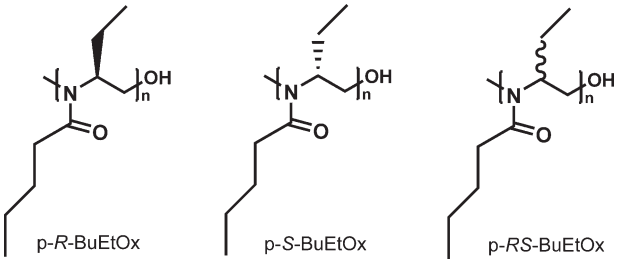

Figure 1. Schematic presentation of the chemical structures of the investigated poly(2-oxazoline)s.

Another class of main-chain chiral polymers are 4- and/or 5-substituted poly(2-oxazoline)s. A previous investigation has shown by combined circular dichroism (CD) and small-angle neutron scattering (SANS) measurements that poly(*R*-2-butyl-4-ethyl-2-oxazoline) (p-*R*-BuEtOx) and p-*S*-BuEtOx form a flexible, dynamic secondary structure in solution while p-*RS*-BuEtOx forms a random coil.[15] However, the bulk properties of such chiral poly(oxazoline)s have only been briefly mentioned in the literature. Optically active poly(2-oxazoline)s were found to be semicrystalline since they reveal a melting peak in the first heating scan while the second heating scan only showed a T_g.[16]

Here, we report the bulk thermal properties of p-*R*-BuEtOx, p-*RS*-BuEtOx, and p-*S*-BuEtOx (Figure 1), including thermal transitions and the influence of annealing on the crystal formation as investigated by differential scanning calorimetry (DSC) measurements and X-ray powder diffraction (XRD). Circular

*Corresponding authors. E-mail: r.hoogenboom@tue.nl (R.H.); ulrich.schubert@uni-jena.de (U.S.S.).

 Published on Web 04/22/2010

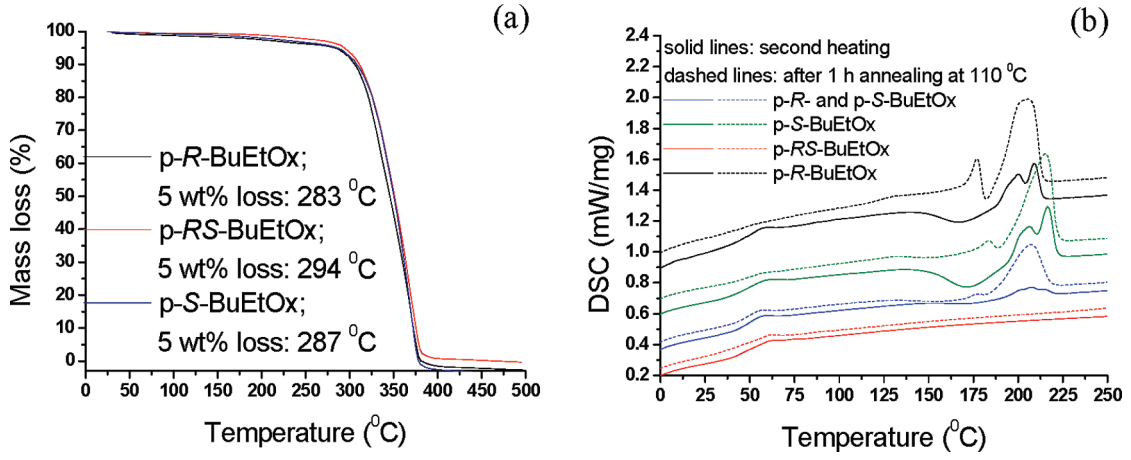

Figure 2. (a) TGA traces of p-*R*-BuEtOx, p-*RS*-BuEtOx, and p-*S*-BuEtOx indicating the temperature at which 5% of the weight was lost. (b) DSC traces of the second heating scan and after annealing the sample for 1 h at 110 °C of p-*R*-BuEtOx, p-*RS*-BuEtOx, p-*S*-BuEtOx, and a 50:50 mixture of p-*R*-BuEtOx and p-*S*-BuEtOx.

Table 1. Thermal Properties Obtained by the DSC Measurements

	second heating run[a]							after annealing[a,b]		
polymer −BuEtOx	T_g (°C)	ΔC_p (J/(g K))	T_{cc} (°C)	ΔH (J/g)	T_{m1} (°C)	T_{m2} (°C)	ΔH (J/g)	T_{m1} (°C)	T_{m2} (°C)	ΔH (J/g)
S	50	0.33	173	12	206	217	15	184	215	30
RS	50	0.34								
R	52	0.36	167	7.1	200	209	10	177	205	35
mixture	46	0.38			207		2.7	174	208	14

[a] Heating rate: 20 °C/min. [b] Annealed at 110 °C for 1 h.

dichroism (CD) measurements were further performed to determine the possible formation of a secondary structure in the crystals.

Experimental Section

P-*R*-BuEtOx, p-*S*-BuEtOx, and p-*RS*-BuEtOx were prepared according to a previously reported procedure.[15] The molar masses (M_n) and polydispersity indexes (PDI) are 4.100 g/mol and 1.27 for p-*R*-BuEtOx used for DSC measurements and 6.140 g/mol and 1.27 for p-*R*-BuEtOx used for XRD measurements, 4.950 g/mol and 1.27 for p-*S*-BuEtOx used for DSC measurements, and 6.850 g/mol and 1.31 for p-*S*-BuEtOx used for XRD measurements and 5.100 g/mol and 1.25 for p-*RS*-BuEtOx, respectively, as determined by size exclusion chromatography (SEC, polystyrene standards).

Thermal transitions were determined on a DSC 204 F1 Phoenix by Netsch under a nitrogen atmosphere with cooling rates of 20 °C/min and heating rates of 20 °C/min. Thermal transitions measured with a heating rate of 1 °C/min were measured on a DSC Q2000 by TA under a nitrogen atmosphere.

X-ray diffraction (XRD) measurements were performed on a Rigaku Geigerflex Bragg−Brentano powder diffractometer as well as on a Bruker D8 discover with GADDS, a two-dimensional (2D) detector, and parallel beam optics. The XRD powder patterns were recorded with the Rigaku apparatus using Cu radiation, wavelength 1.540 56 Å, at 40 kV and 30 mA. The scans were performed with a 0.02 step in 2Θ and a dwell time of 1.5 s. The samples were mounted with Vaseline, pure petroleum jelly, as a powder on a glass plate. The 2D diffraction patterns were obtained with the Bruker system using Cu radiation, wavelength 1.541 84 Å, at 40 kV and 40 mA and a exposure time of 20 min. In this case the samples were prepared in a glass capillary and heated with a Linkam system, TMS94, to elevated temperatures.

CD spectra were measured on a Jasco J815 spectropolarimeter equipped with a Linkam temperature controller for temperatures ranging from 20 to 250 °C. The samples were spin coated from chloroform (40 mg/mL) on a quartz glass for 2 min with 2000 rpm. The following scanning conditions were used: 50 nm/min scanning rate; 1 nm bandwidth; 0.1 nm data pitch; 0.5 s response time; and 10 accumulations. The melting curve was obtained by heating the sample with 1 °C/min.

Results

The thermal properties of the enantiopure and racemic poly(2-oxazoline)s were measured by DSC from −30 to 250 °C with a heating rate of 20 °C/min. From the thermal gravimetric analysis (TGA) measurements (Figure 2a) it was observed that these polymers are stable up to at least 250 °C. In the first heating run, the enantiopure poly(2-oxazoline)s revealed a glass transition temperature (T_g) followed by cold crystallization (T_{cc}) and double melting peaks (T_{m1} and T_{m2}) while the racemic polymer only revealed a T_g. The DSC results from the second heating run are shown in Figure 2b and summarized in Table 1. All polymers have approximately the same glass transition temperature (T_g) around 50 °C with a heat capacity (ΔC_p) of about 0.3 J/(g K). However, the enantiopure polymers show an exothermic crystallization (T_{cc}) due to cold crystallization and two melting peaks (T_{m1} and T_{m2}) in the second heating run, while the racemic polymer does not. The cooling rate of 20 °C/min was obviously too fast for the enantiopure polymers to completely crystallize from the melt, and therefore, the crystallization takes place from the rubbery state during the heating run. In general, double melting transitions can be explained by three major proposed mechanisms, namely melt-recrystallization, dual lamellae population, and dual crystal structures.[17] The thermal behavior of the polymers was further investigated after annealing above the T_g at 110 °C for 1 h. Then, the polymer crystallizes and the cold-crystallization exotherm is eliminated in p-*R*-BuEtOx and almost completely disappeared in p-*S*-BuEtOx (Figure 2b). Again, two melting peaks are observed. The first melting endotherm (T_{m1}) is probably the result of crystals formed during annealing, and the second melting peak (T_{m2}) is broad and is probably a combination of T_{m1} and T_{m2} that were observed in the second heating

scan. The melt enthalpy (ΔH_m) increased after annealing, which means that the crystallinity of the enantiopure polymers is increased after the thermal treatment. After annealing, still no melting peak appears for the racemic polymer, indicating its amorphous behavior. The melting peaks observed for the enantiopure polymers might be due to melting of polymer crystals containing an ordered chiral structure, which might be helices or ordered arrays of helices, while the racemic polymer forms an unordered amorphous structure.

When a 50:50 mixture of both enantiopure polymers is measured with DSC, ΔH_{cc}, and ΔH_m are much lower during the second heating run compared to the individual enantiopure polymers (Figure 2b), which indicates a partial prevention of crystallization after mixing. However, the formation of some kind of superstructure upon mixing, similar to the stereocomplexes formed by poly(L-lactide) and poly(D-lactide), might be possible.[18,19] Alternatively, the presence of both enantiomers could obstruct the formation of crystals of single enantiomers, resulting in a smaller crystalline fraction. After annealing, ΔH_m is increased but still not to the same extent as the individual enantiopure polymers.

The melting behavior of p-*S*-BuEtOx was further investigated by varying the heating rate between 10 and 70 °C/min and by annealing the sample at different temperatures ranging from 110 to 180 °C for 1 h. The results, summarized in Table 2 and in Figure 3a, reveal that T_{m1} is shifting to higher temperatures with increasing heating rate, while T_{m2} stays at the same temperature. Moreover, the ratio of ΔH_{m1}:ΔH_{m2} increases until only one melting peak is observed. These results indicate that the two melting peaks are caused by melt-recrystallization.[17,20] According to the melt-recrystallization mechanism, the first melting peak is caused by the initially formed crystals, which recrystallize into more perfect crystals that are responsible for the second melting peak. During the heating run, melting and recrystallization are competitive, and therefore, recrystallization is suppressed when the heating rate is increased. This results in a smaller fraction of recrystallized crystals until only one melting peak is observed. Such a behavior is also observed, for example, in syndiotactic polypropylene (sPP) if the stereoregularity is relatively low (rrrr < 90%).[7] In that case a double melting peak is observed in the DSC trace, whereby the first melting peak is due to the partial melting of irregular crystals in the disordered helical form followed by successive recrystallization into the more ordered helical form which melts at higher temperatures, causing the second melting peak.[7] Therefore, it is also possible that p-*S*-BuEtOx initially forms crystals with a disordered secondary structure that recrystallize during melting into crystals with a more defined secondary structure.

Furthermore, T_{cc} is shifted to higher temperatures with increasing heating rate and ΔH_c is decreasing until no T_{cc} is observed anymore. Less time is available for cold-crystallization with a higher heating rate, which causes this shift of T_{cc} to higher temperatures and a decrease in enthalpy. Since fewer crystals are formed with the increase in heating rate, ΔH_m also decreases in intensity.

The annealing temperature further influences the thermal properties as illustrated in Table 3 and Figure 3b. With the increase in annealing temperature from 110 to 180 °C, T_{m1} shifts to higher temperature and increases in intensity, while T_{m2} remains around the same temperature and decreases in intensity. Although still two melting peaks are present after annealing at 180 °C for 1 h, such a shift in T_m and change in ΔH_m was also observed for PLLA, where both melting peaks relate to the helical α-form[12,13] and also to the helical comb polymer PLLA.[21] The authors attributed the double melting peaks to melt-recrystallization. It seems that with increasing annealing temperature more initial crystals are formed that cause an increase in ΔH_{m1}. These initial crystals are more perfect, which causes the increase in T_{m1}. Another indication that the second melting peak is due to melt-recrystallization is the dip between the two melting endotherms present after annealing the sample at 120−150 °C.[16]

Table 2. Thermal Properties of p-*S*-BuEtOx Obtained by DSC at Different Heating Rates

heating rate (°C/min)	T_{cc} (°C)	ΔH_{cc} (J/g)	T_{m1} (°C)	T_{m2} (°C)	ΔH_m (J/g)
10	158	21	195	215	37
20	173	12	206	217	15
30	176	1.9	208	215	3.9
40			208	215	2.7
50			208	214	2.0
60				214	1.3
70				214	1.2

Table 3. Thermal Properties Obtained by DSC after Annealing p-*S*-BuEtOx at Different Temperatures for 1 h

$T_{annealing}$ (°C)	T_{cc}[a] (°C)	ΔH_{cc}[a] (J/g)	T_{m1} (°C)	T_{m2} (°C)	ΔH_m (J/g)
110			184	215	30
120	191	0.9	185	213	43
130	193	1.1	188	211	32
140	197	1.2	192	213	43
150	200	1.1	194	214	40
160			198	215	39
170			202	216	38
180			206	217	36

[a] Exothermic dip between two melting peaks.

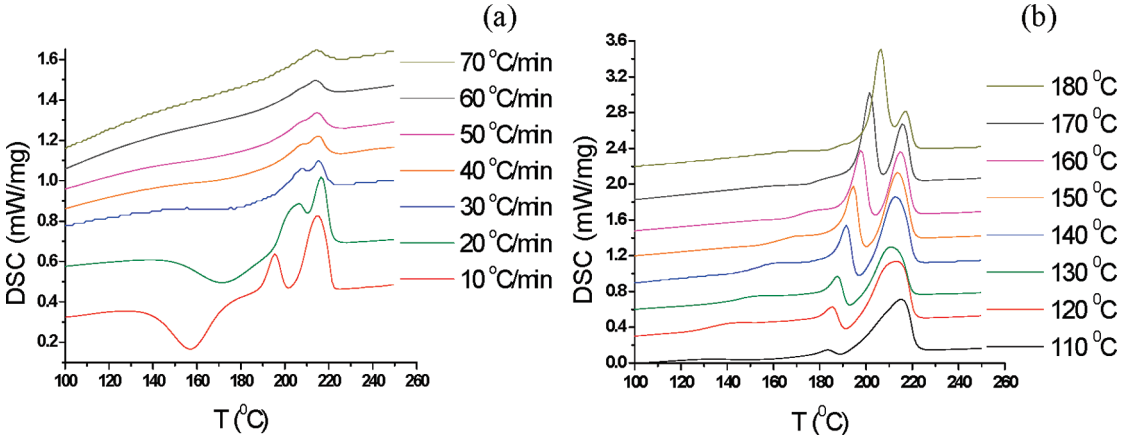

Figure 3. DSC traces of p-*S*-BuEtOx (a) of the second heating run at different heating rates and (b) after annealing at different temperatures for 1 h (heating rate: 20 °C/min).

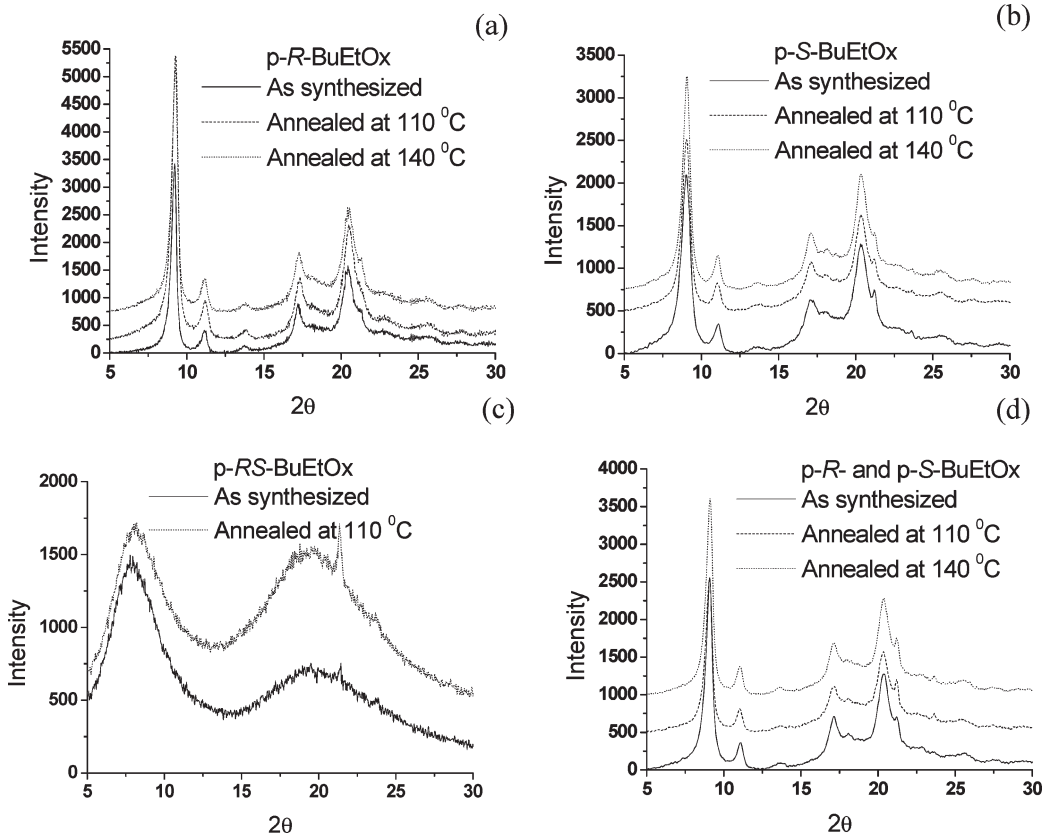

Figure 4. XRD patterns of (a) p-*R*-BuEtOx, (b) p-*S*-BuEtOx, (c) p-*RS*-BuEtOx, and (d) 50:50 mixture of p-*R*-BuEtOx and p-*S*-BuEtOx, before and after annealing.

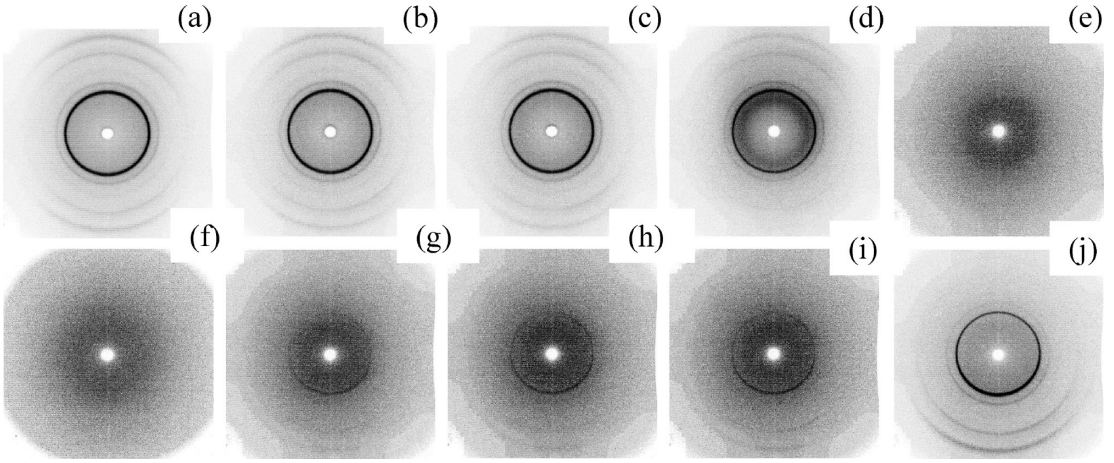

Figure 5. XRD 2D patterns of p-*R*-BuEtOx during heating and cooling: (a) room temperature (RT), (b) 100 °C, (c) 150 °C, (d) 225 °C first measurement, (e) 225 °C second measurement, (f) 250 °C, (g) 175 °C, (h) 150 °C, (i) 100 °C, (j) RT.

X-ray diffraction (XRD) measurements were performed on p-*R*-BuEtOx and p-*S*-BuEtOx powders before and after annealing at 110 and 140 °C to investigate if the polymers are already crystalline after synthesis and if the crystal structure changes upon annealing. For comparison, also p-*RS*-BuEtOx was analyzed with XRD before and after annealing at 110 °C. Figure 4a,b demonstrates that the enantiopure polymers are obtained as semicrystalline materials after synthesis and purification. No significant change is observed in the XRD pattern after annealing at 110 or 140 °C, indicating that the crystal structure does not change after the thermal treatment. The diffraction peaks correspond to a *d*-spacing of 9.7, 7.9, 6.5, 5.2, 4.3, and 3.4 Å. P-*RS*-BuEtOx (Figure 4c) shows broad bands before and after annealing, indicating that this polymer is amorphous. The broad peak between 2Θ of 15° and 30° with sharp peaks on top arises from the Vaseline that was used for the sample preparation and is also present in the XRD patterns of the enantiopure polymers. The XRD of the 50:50 mixture of p-*S*-BuEtOx and p-*R*-BuEtOx revealed the same crystal structure compared to the separate enantiopure polymers. Also after thermal treatment the crystal structure of the mixture does not change, indicating that no stereocomplexes are formed.

Furthermore, the 2D XRD patterns of the p-*R*-BuEtOx powder were measured at different temperatures to investigate if the crystalline structure changes upon heating. From Figure 5 it can be seen that the polymer was initially semicrystalline at room

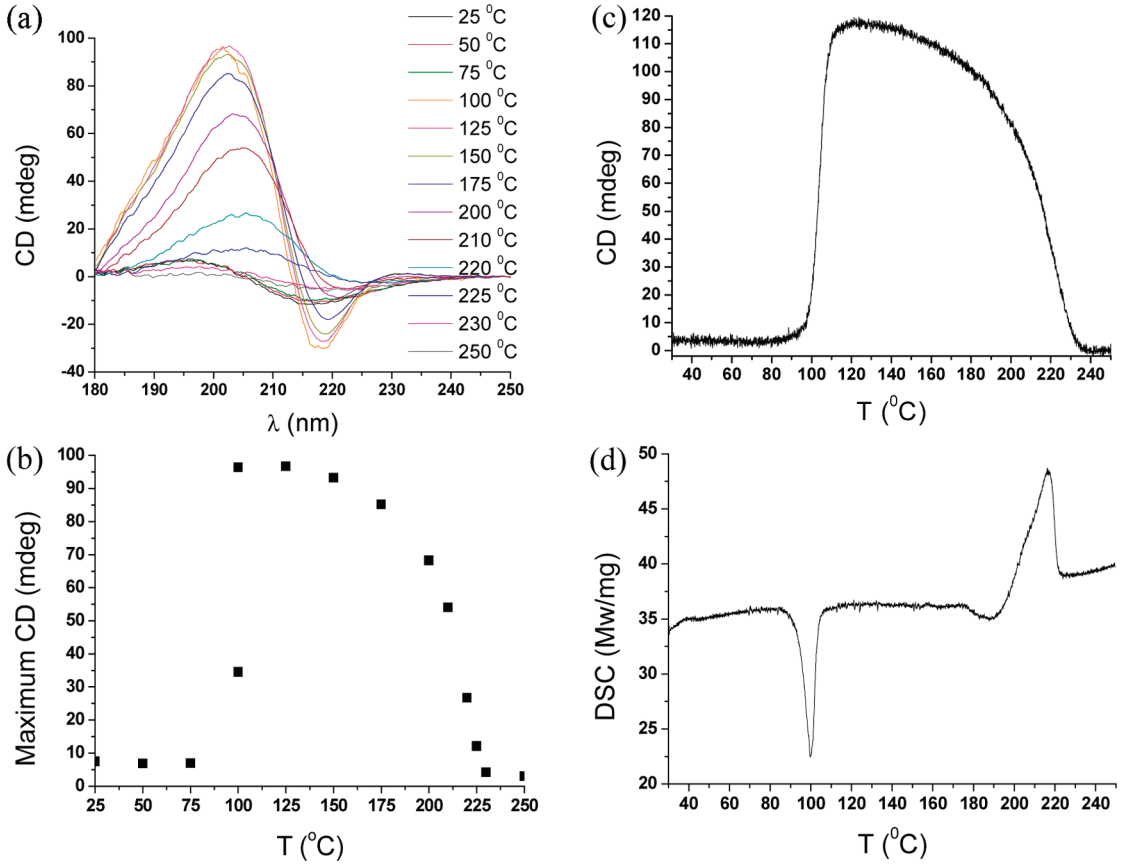

Figure 6. (a) CD spectra of p-*R*-BuEtOx spin-coated on quartz glass at different temperatures. (b) CD maxima obtained from (a) plotted against temperature. (c) Melting curve of p-*R*-BuEtOx obtained with CD at a wavelength of 202 nm (heating rate: 1 °C/min). (d) First heating scan of p-*R*-BuEtOx obtained by DSC (heating rate: 1 °C/min).

temperature (Figure 5a) and that the crystalline structure does not change upon heating up to 200 °C. At 225 °C, the polymer starts to become amorphous (Figure 5d), and during the second measurement at 225 °C, the polymer was completely amorphous (Figure 5e). These results confirm that the double melting peak is caused by the melt-recrystallization mechanism and not due to the presence of a second crystalline structure. Upon slow cooling, the polymer crystallizes again down to 100 °C. By further decreasing the temperature to room temperature, the crystallization occurs faster and the final crystalline fraction is similar to the initial sample before heating.

To determine if the melting peaks are the result of the melting of crystals that contain an ordered chiral structure, circular dichroism (CD) measurements were carried out on a thin polymer film spin-coated on a quartz slide. CD spectra of the polymer film were taken at different temperatures starting at 25 °C up to 250 °C (Figure 6a,b). Below 100 °C, only a small dichroic Cotton effect was observed, indicating that only a minor fraction of the polymer is present in an ordered chiral structure. However, when the temperature reached 100 °C, a significant increase in the Cotton effect around 200 nm was observed, indicating the formation of an ordered chiral structure at this temperature. With the further increase in temperature up to 150 °C, the Cotton effect remains constant and decreases again with increasing in temperature until almost no Cotton effect was observed at 230 °C, meaning that the ordered chiral structure disappeared. Even though the CD results clearly show the formation of an ordered chiral structure, it cannot be assigned to a certain type of secondary structure due to the absence of model compounds.

In order to compare the DSC results with the CD results, a melting curve of the polymer was measured by both techniques using a heating rate of 1 °C/min (Figure 6c,d). Since the maximum Cotton effect stays around 202 nm in the CD spectra over the whole temperature range, the CD melting curve was recorded at this wavelength. By comparing the DSC with the CD results, it is evident that the Cotton effect increases significantly during the cold crystallization, which is indicated by a dip in the DSC trace at 100 °C. This means that during cold crystallization crystals are formed, which contain an ordered chiral structure. In addition, the melting peaks observed in the DSC trace can be related to the melting of this ordered chiral structure into a disordered melt, since the Cotton effect completely disappears at a temperature just above the end of the melting endotherms.

Conclusions

The enantiopure poly-*R*-BuEtOx and p-*S*-BuEtOx are semicrystalline polymers with T_g values around 50 °C and double melting peaks caused by melt-recrystallization, which were determined by DSC measurements. In the second heating run, an exothermic dip was observed in the DSC thermograph due to cold crystallization, which could not be observed anymore after annealing the polymer. In contrary, the racemic p-*RS*-BuEtOx is amorphous with a similar T_g around 50 °C. The XRD measurements confirmed that the enantiopure polymers are semicrystalline and that the crystal structure does not significantly change after annealing. Furthermore, the XRD measurements reveal that the crystal structure does not change during heating, which confirms that the double melting peaks found with DSC are due to the melt-recrystallization mechanism.

By comparing the DSC data with the CD data, it was concluded that the crystals formed in the enantiopure polymer

contain an ordered chiral structure. Therefore, it was proposed that these chiral poly(2-oxazoline)s initially form disordered chiral structures that recrystallize during melting into a more perfect chiral structure. Upon further heating, these crystals melt into a disordered structure.

The amount of crystallization and type of crystals formed in the chiral poly(2-oxazoline)s can be controlled by the thermal history. This has a direct influence on the formation of the ordered chiral structure.

Acknowledgment. The authors thank the Dutch Polymer Institute (DPI) for financial support, Wilco Appel for the help with the Linkam heating stage and the CD instrument, and Dr. Stephanie Hornig for helpful comments.

References and Notes

(1) Wunderlich, B. *Prog. Polym. Sci.* **2003**, *28*, 383–450.
(2) Yamamoto, T.; Sawada, K. *J. Chem. Phys.* **2005**, *123*, 234906/1–12.
(3) Hoogenboom, R. *Angew. Chem., Int. Ed.* **2009**, *48*, 7978–7994.
(4) Hoogenboom, R.; Fijten, M. W. M.; Thijs, H. M. L.; van Lankvelt, B. M.; Schubert, U. S. *Des. Monomers Polym.* **2005**, *8*, 659–671.
(5) Litt, M.; Rahl, F.; Roldan, L. G. *J. Polym Sci., Part A-2* **1969**, *7*, 463–473.
(6) Arranz-Andrés, J.; Peña, B.; Benavente, R.; Pérez, E.; Cerrada, M. L. *Eur. Polym. J.* **2007**, *43*, 2357–2370.
(7) De Rosa, C.; Auriemma, F. *Prog. Polym. Sci.* **2006**, *31*, 145–237.
(8) Vanegas, M. A. E.; Quijada, R.; Serafini, D.; Galland, G. B.; Palza, H. *J. Polym. Sci., Part B: Polym. Phys.* **2008**, *46*, 798–806.
(9) Jones, T. D.; Chaffin, K. A.; Bates, F. S.; Annis, B. K.; Hagaman, E. W.; Kim, M.-H.; Wignall, G. D.; Fan, W.; Waymouth, R. *Macromolecules* **2002**, *35*, 5061–5068.
(10) Chen, C.-M.; Hsieh, T.-E.; Ju, M.-Y. *J. Alloys Compd.* **2009**, *480*, 658661.
(11) Zhang, J.; Duan, Y.; Sato, H.; Tsuji, H.; Noda, I.; Yan, S.; Ozaki, Y. *Macromolecules* **2005**, *38*, 8012–8021.
(12) Pan, P.; Kai, W.; Zhu, B.; Dong, T.; Inoue, Y. *Macromolecules* **2007**, *40*, 6898–6905.
(13) Zhang, J.; Tashiro, K.; Tsuji, H.; Domb, A. J. *Macromolecules* **2008**, *41*, 1352–1357.
(14) Hirata, M.; Kimura, Y. *Polymer* **2008**, *49*, 2656–2661.
(15) Bloksma, M. M.; Rogers, S.; Schubert, U. S.; Hoogenboom, R. *Soft Matter* **2010**, *6*, 994–1003.
(16) Guo, X. G.; Schulz, R. C. *Polym. Int.* **1994**, *34*, 229–233.
(17) Ling, X. Y.; Spruiell, J. E. *J. Polym. Sci., Part B: Polym. Phys.* **2006**, *44*, 6898–6905.
(18) He, Y.; Xu, Y.; Wei, J.; Fan, Z.; Li, S. *Polymer* **2008**, *49*, 5670–5675.
(19) Wang, Y.; Mano, J. F. *J. Appl. Polym. Sci.* **2008**, *107*, 1621–1627.
(20) Ling, X.; Spruiell, J. E. *J. Polym. Sci., Part B: Polym. Phys.* **2006**, *44*, 3378–3391.
(21) Zhao, C.; Wu, D.; Huang, N.; Zhao, H. *J. Polym. Sci., Part B: Polym. Phys.* **2008**, *46*, 589–598.